

Aquatic and Soil CO₂ Emissions from forested wetlands of Congo's Cuvette Centrale

Antoine de Clippele^{1*}, Astrid C. H. Jaeger^{1*}, Simon Baumgartner^{2,3}, Marijn Bauters⁴, Pascal Boeckx⁵, Clement Botefa⁶, Glenn Bush⁷, Jessica Carilli¹, Travis W. Drake¹, Christian Ekamba⁸, Gode Lompoko⁶, Nivens Bey Mukwiele⁶, Kristof Van Oost³, Roland A. Werner¹, Joseph Zambo⁷, Johan Six¹, Matti Barthel¹

1 Department of Environmental Systems Science, ETH Zurich, Switzerland

2 Research Division Agroecology and Environment, Agroscope, Zurich, Switzerland

3 Earth and Life Institute, Université Catholique de Louvain, Louvain-la-Neuve, Belgium

4 Q-ForestLab, Department of Environment, Ghent University, Belgium

5 Isotope Bioscience Laboratory, Department of Green Chemistry and Technology, Ghent University, Belgium

6 ICCN Jardin de Botanique d'Eala, Mbandaka, Democratic Republic of Congo

7 Woodwell Climate Research Center, USA

8 Coordination Provinciale de l'environnement, Mbandaka, Democratic Republic of Congo

*These authors contributed equally to this study.

Correspondence to: Antoine de Clippele (antoine.declippele@usys.ethz.ch)

Field Code Changed

Abstract. Within tropical forest ecosystems, wetlands such as swamp forests are an important interface between the terrestrial and aquatic landscape. Despite this assumed importance, there is a paucity of carbon flux data from wetlands in tropical Africa. Therefore, the magnitude and source of carbon dioxide (CO₂) fluxes, carbon isotopic ratios, and environmental conditions were measured for three years between 2019 to 2022 in a seasonally flooded forest and a perennially flooded forest in the *Cuvette Centrale* of the Congo Basin. The mean surface fluxes for the seasonally flooded site and the perennially flooded site were $2.36 \pm 0.51 \mu\text{mol m}^{-2} \text{s}^{-1}$ and $4.38 \pm 0.64 \mu\text{mol m}^{-2} \text{s}^{-1}$ respectively. The time series data revealed no ~~discernible-obvious~~ seasonal pattern in CO₂ fluxes. As for the environmental drivers, the fluxes at the seasonally flooded site exhibited a positive correlation with soil temperature and soil moisture. Additionally, the water ~~table-depth~~level appeared to be a significant factor, demonstrating a quadratic relationship with the soil fluxes at the seasonally flooded site. $\delta^{13}\text{C}$ values showed a progressive increase across the carbon pools, from above-ground biomass, then leaf litter, to soil organic carbon (SOC). However, there was no significant difference in $\delta^{13}\text{C}$ enrichment between SOC and soil respired CO₂. This lack of enrichment can be attributed to either a significant contribution from the autotrophic component of soil respiration or a result of closed system dynamics.

An *in-situ* derived gas transfer velocity ($k_{600} = 2.95 \text{ cm h}^{-1}$) was used to calculate the aquatic CO₂ fluxes at the perennially flooded site. Despite the low k_{600} , relatively high CO₂ surface fluxes were found due to very high partial pressure of CO₂ (pCO₂) values measured in the flooding waters. Overall, these results offer a quantification of the CO₂ fluxes from forested wetlands and provide an insight of the temporal variability of these fluxes as well as their sensitivity to environmental drivers.

Formatted: Subscript

1 Introduction

Along with the oceans and Northern Hemisphere forests, tropical forests represent one of the three main components of the global carbon sink (Mitchard 2018). However, due to relatively high gross primary productivity, temperature and soil moisture, tropical forest soils also constitute a large terrestrial source of carbon dioxide (CO₂). Indeed, tropical regions are estimated to contribute up to 64% ~~of the~~ global soil respiration, rendering it as the largest flux of CO₂ from terrestrial ecosystems to the atmosphere (Hashimoto et al. 2015; Huang et al. 2020).

Wetland cover in the tropical Congo Basin is estimated to range between 332,620 and 359,556 km² (Bwangoy et al. 2010; Fatras et al. 2021). This area includes the *Cuvette Centrale*, which spans approximately 167,600 km² and hosts lowland and swamp forests, including the largest peatland complex across the tropics (Crezee et al. 2022). With catchment drainage from north and south of the equator as well as sustained rainfall at the center of the basin (Runge 2007; Breitengroß 1972), the *Cuvette Centrale* shows near permanent inundation. Characterizing CO₂ fluxes in this extensive region is especially important since inland waters are increasingly recognized as significant sources of greenhouse gases (GHG) within the terrestrial landscape (Bastviken et al. 2011; Drake, Raymond, and Spencer 2018; Borges, Darchambeau, et al. 2015; Rosentreter et al. 2021) and notably in ~~the~~ global carbon dioxide emissions (Raymond et al. 2013). Recent data additionally suggests that the Congo Basin’s inland waters might emit more carbon (C) per area than their counterparts in the Amazon Basin (Alsdorf et al. 2016). Profound hydrological (Alsdorf et al. 2016), structural (Lewis et al. 2013), ecological (Slik et al. 2015; Parmentier et al. 2007), aquatic biogeochemical (Borges, Abril, et al. 2015), and terrestrial biogeochemical (Hubau et al. 2020) differences indicate that GHG flux estimates cannot simply be transferred from the Neotropics to the Afro-tropics. However, while recent research on GHG emission from the Congo Basin has focused on either riverine (Bouillon et al. 2012; Paul J. Mann, Tfaily, et al. 2014; Upstill-Goddard et al. 2017; Borges et al. 2019) or terrestrial fluxes (Baumgartner et al. 2020; Gallarotti et al. 2021; Barthel et al. 2022; Daelman et al. 2024), direct measurements from forested wetlands are still lacking. Despite its immense global importance, only two studies, to the best of our knowledge, have been looking into GHG emissions from Congo’s wetlands (Tathy et al. 1992; Barthel et al. 2022; ~~Daelman et al. 2024~~).

Forested wetlands/swamp forests are located at the transition zone between the terrestrial and the aquatic realm. The duration and seasonality of the flooding in the forests will constrain the contribution from/to the river system. While flooded, the swamp forests are connected to the river system and receive and/or discharge materials from/to the river network (Aufdenkampe et al.

Formatted: French (Switzerland)

Formatted: Font color: Auto

Formatted: Font color: Auto

65 2011). Variations of riverine greenhouse gas concentrations have been shown to be driven by fluvial-wetland connectivity for
the *Cuvette Centrale* based on data from 10 expeditions across the Congo River network (Borges et al. 2019). Furthermore,
streams and rivers draining Congo's flooded forests were found to have the highest dissolved concentrations of CO₂ among
different land cover types in the Basin, indicating the substantial contribution of forested wetlands on the overall inland water
GHG budget (Paul J. Mann, Spencer, et al. 2014).

70

Here, we report three years of carbon dioxide (CO₂) fluxes measured from two sites situated within the *Cuvette Centrale*: a
seasonally flooded forest site and a perennially flooded forest site. During the observation period, surface CO₂ fluxes whether
soil or aquatic, were measured fortnightly to capture the seasonal and inter-annual variation of the fluxes. ~~Additionally, at the
seasonally-flooded site, environmental parameters (temperature, soil moisture and water table level) were monitored and their
effects on the soil fluxes quantified. At the perennially flooded site, the carbon to nitrogen ratio (C:N), dissolved organic
carbon (DOC) and pH were also measured to investigate their potential effect on CO₂ fluxes.~~ Hence, these results provide
insights into the temporal dynamics of CO₂ fluxes in forested wetlands across two different flooding regimes.

75

2 Materials and Methods

2.1 Study sites

80 The sites were located near the town of Mbandaka (Democratic Republic of the Congo, Équateur province), which is located
at the Ruki-Congo confluence within the *Cuvette Centrale* (Figure 2). The mean annual precipitation and mean annual
temperature of the sampling area are 1588 mm and 25 °C, respectively (see the measurements detailed below). The long dry
season in Mbandaka typically lasts from July to August, while the short dry season occurs between January and February.
Here, surface CO₂ fluxes were measured at two different sites across two different hydrological regimes, one in a seasonally
85 flooded forest (N 0.06335, E 18.31054, 300 m a.s.l.) – referred to as SFF site –and in a perennially flooded forest (S 0.03135,
E 18.3102, 305 m a.s.l.) – referred to as PFF site (Figure 1).

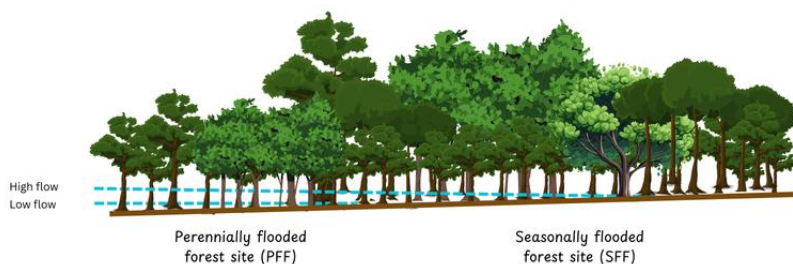


Figure 1. Diagram showing the location of the two experimental sites (PFF and SFF) relative to the hydrological gradient.

90 The seasonally flooded forest site (SFF) investigated was located within a botanical garden 7 km from the center of Mbandaka (*Jardin Botanique d'Eala*, operated by the *Institute Congolais pour la Conservation de la Nature* (ICCN)). The botanical garden comprises 371 ha of land consisting of 35% dense swamp forest, 14% forest on firm ground, 32% open forest, and the remaining area consisting of secondary forest, grassland, and deforested land, of which 189 ha are protected forest area. There are 3500 different trees and herbaceous plant species, with the main tree species being *Hevea brasiliensis*, *Ouratea arnoldiana*,
 95 *Pentaclethra eetveldeana*, *Strombosia tetandra*, and *Daniella pynaertii*. The soil at the site, covered by a thick litter layer, was characterized as Eutric Gleysols (texture 42/50/8 sand/silt/clay in %, bulk density 1.27 g cm⁻³). The litter layer harbors a dense mesh of fine roots, whereas almost no roots were found to penetrate the upper mineral soil layer (0-30 cm). ~~The SFF site is seasonally flooded from about December to January (~ 2 months). The SFF site is seasonally flooded during the rainy season from about December to January (~ 2 months).~~

Formatted: Font color: Auto

100

~~At the SFF site, combined soil moisture and temperature sensors (ECH₂O 5TM, Meter Group, Inc. USA) connected to loggers (Em50, Meter Group, Inc., USA) were installed at 10 and 30 cm depth, respectively. The data was recorded every 6 h. At the SFF site, combined soil moisture and temperature sensors (ECH₂O 5TM, Meter Group, Inc. USA) connected to loggers (Em50, Meter Group, Inc., USA) were installed at 30 cm depth, and data was recorded every 6 h. Unfortunately, one logger was stolen and the other logger stopped working during deployment; thus, data is only available from November 2019 to July 2020 (Figure 3Figure 3). Afterward, TMS-4 dataloggers (TOMST, Czechia) were installed in December 2020 to record surface volumetric soil water content (0-14cm) and soil temperature at 8 cm depth in 15-minute intervals. In addition, TMS-4 dataloggers (TOMST, Czechia) were installed in December 2020 to record volumetric soil water content and soil temperature in 15 minute intervals.~~ Raw data (soil moisture count) retrieved from TMS-4 dataloggers was converted into soil VWC with calibrations curves, following Wild et al. (2019), using site-specific soil properties (soil texture: 42/50/8 sand/silt/clay in %, bulk density 1.27 g cm⁻³) and measured soil temperatures. The soil VWC values from the ECH₂O 5TM sensors showed a systematic offset compared to those obtained from the TMS-4 dataloggers. This was attributed to instrument artefact and corrected by using the difference between maximum values. Furthermore, precipitation, air temperature, relative humidity, solar radiation, and wind

Formatted: Font color: Auto

105

Formatted: Font color: Auto

110

speed data were retrieved for the observation period from the Trans-African Hydro-Meteorological Monitoring Observatory
115 (TAHMO) station located in close vicinity to the forest site (ATMOS 41, Meter Group, Inc., USA).

The perennially flooded forest (PFF) site is located about 8 km upstream of the Congo-Ruki confluence, following a small
side tributary named Lolifa. The headwater stream area is completely flooded for most of the year, making the stream bed
channel indistinguishable. This creates a continuous wetland area where the PFF site is located. While the water is mostly
120 stagnant at the site, a small drainage flow appears during the dry season (late June to early September). The site was accessed
with a motorized dugout canoe, and sampling was done fortnightly from the side of the canoe. The main tree species at the
PFF site were *Uapaca sp*, *Irvingia mitii*, and *Daniella pynaertii* De Wild. Additional to the surface CO₂ fluxes, water samples
were collected on the same day to measure pH, dissolved organic carbon (DOC) and total dissolved nitrogen (TDN). The
presented C:N ratio was thus calculated using TDN rather than dissolved organic nitrogen (DON). Previous analyses (Drake
125 et al. 2023) showed that TDN consistently comprised an average of 90% of DON and thus reflected well the relative changes
of DON concentrations. The specific methods used for sample processing and analysis as well as the calculations are described
in Drake et al., (2023).

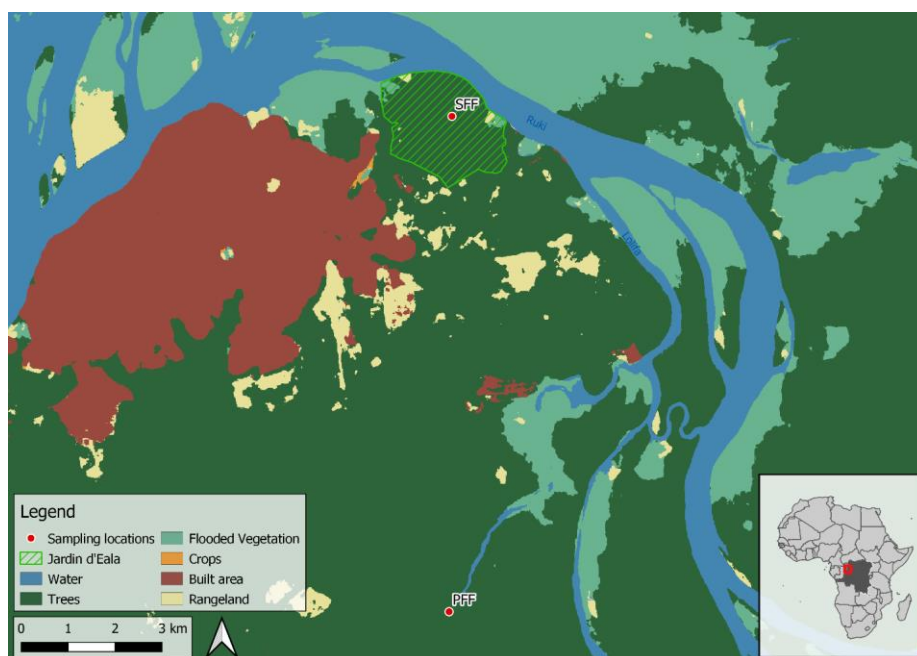


Figure 2. Map presenting the two sampling sites in the vicinity of Mbandaka (Democratic Republic of the Congo). The boundaries of the Jardin botanique d'Eala are highlighted. Map data: © 2020-2023 Impact Observatory, Inc. and GADM.

2.2 CO₂ fluxes

2.2.1 CO₂ surface fluxes at the SFF site

A total of six polyvinylchloride soil flux chambers (height = 0.3m, diameter = 0.3m) were installed in November 2019 at the SFF site. The chamber bases were inserted approximately 5 cm into the ground and remained in place throughout the measurement period, with the chambers left open except during sampling. Chambers affected by seasonal flooding were measured for as long they were not completely submerged at which point floating chambers (V = 17L) were used instead. Sampling with the soil chambers was conducted fortnightly for three consecutive years (2019/11 – 2022/12), totalling 403 flux measurements. Sampling was interrupted once for about six months due to logistical constraints (first half of 2022).

Each chamber lid was equipped with a thermocouple to measure headspace temperature, a vent tube to avoid pressure changes, and a sampling port. The sampling port had a 3-way Luer valve attached, connecting the syringe, needle, and chamber. Before

Formatted: Font color: Auto

withdrawing each gas sample from the headspace, chamber air was mixed by moving the syringe plunger several times; for
145 soil GHG flux determination, gas samples were taken at timesteps of 20 min throughout 1 hour (t1 = 0 min, t2 = 20 min, t3 =
40 min, t4 = 60 min). A longer chamber closure time than recommended (Pavelka et al. 2018) was used to obtain robust
Keeling plots along with the flux measurements. At each timestep, 20 mL of gas sample were stored in 12 mL pre-evacuated
vials (Labco, UK) using a gas-tight disposable plastic syringe (20 mL). The resulting vial overpressure prevents air ingress
due to temperature and pressure changes potentially occurring during transport and is required for sample withdrawal by the
150 GC autosampler. To aid vacuum and sample preservation, each evacuated vial was sealed with an additional silicone layer
(Dow Corning 734, Dow Silicones Corporation, USA). Soil CO₂ fluxes were calculated via linear concentration increase over
time using the ideal gas law $PV = nRT$:

$$n = \frac{PV}{RT} \quad (1) \quad \text{and} \quad F = \frac{\Delta n}{\Delta t} S^{-1} \quad (2)$$

155 with n moles of gas [mol], P partial pressure of trace gas [atm $\mu\text{mol mol}^{-1}$], R gas constant 0.08206 [L atm K⁻¹ mol⁻¹], T
headspace temperature [K], F flux of gas [$\mu\text{mol m}^{-2} \text{s}^{-1}$], $\frac{\Delta n}{\Delta t}$ rate of change in concentration [mol s⁻¹], V chamber volume [L],
and S surface area enclosed by chamber [m²]. The coefficient of determination (r^2) for the linear regression of CO₂ yielded a
 $r^2 > 0.95$ for 95% of the data (Supp. Fig. 1). All data with $r^2 > 0.1$ was kept for the statistical analyses. Such a low r^2 threshold
was maintained because fluxes with low r^2 values are typically related to low flux rates rather than due to methodological or
160 technical issues. Increasing the threshold would introduce a bias toward higher fluxes in the data.

2.2.2 Aquatic surface fluxes at the PFF site

The aquatic surface flux to the atmosphere (F_{CO_2} , $\mu\text{mol m}^{-2} \text{s}^{-1}$) from the PFF site was estimated according to a simple gas
transfer model (Mann et al. 2014):

165 $F_{\text{CO}_2} = k_x \cdot K_H \cdot (p\text{CO}_{2w} - p\text{CO}_{2a}) \quad (3)$

where k_x is the freshwater gas transfer velocity of CO₂ [m s⁻¹], K_H is the Henry's constant for CO₂ [mol m⁻³ atm⁻¹], $p\text{CO}_{2w,a}$ the
partial pressure of CO₂ in water and atmosphere, respectively [μatm].

Since the magnitude of the gas transfer velocity is governed by numerous factors (e.g., wind speed, water current velocity,
170 slope), an *in-situ* gas transfer velocity k was calculated as 3.5 cm h⁻¹ using the aquatic fluxes from the SFF site sampled between
2022-07 to 2022-12 with the above-mentioned floating chamber ($V = 17 \text{ L}$) and the corresponding dissolved CO₂
concentrations of the inundation water at the same site. The value of 3.5 cm h⁻¹ was then applied to the perennially flooded
forest dataset where no floating chamber measurements existed. Hence, fluxes from the PFF site were derived using the
measured gas transfer velocity from the SFF site (3.5 cm h⁻¹).

Formatted: Font color: Auto

Formatted: Font color: Auto

Formatted: Font color: Auto

Formatted: Font color: Auto

Formatted: Font color: Auto

175 In order to compare the *in-situ* derived velocity k_x with the temperature normalized transfer velocity (k_{600}) for tropical wetlands
of 2.4 cm h⁻¹ (Aufdenkampe et al. 2011), we used the equation from Pelletier et al. (2014) to convert k_x to k_{600} .

$$k_x = k_{600} \left(\frac{S_c}{600} \right)^{-b} \quad (4)$$

180 Where S_c is the gas specific Schmid number and b derived from literature (0.66 for wind speed ≤ 3 m/s; Pelletier et al. 2014).
The gas specific Schmid number is a function of water temperature (T in °C) as defined by Wanninkhof (2014):

$$S_{cCO_2} = 1923.6 - 125.06T + 4.3773T^2 - 0.085681T^3 + 0.00070284T^4 \quad (5)$$

185 For pCO_{2a} , the tropospheric mean value from the year 2020 (400 μ atm) was used while pCO_{2w} was determined using the
headspace equilibration technique. That is, 6 mL of bubble-free water sample were injected with a syringe into a 12 mL N₂-
pre-flushed vial (Exetainer®, Labco, UK) pre-poisoned with 50 μ L of 50% ZnCl₂ to stop the microbial activity. After sufficient
equilibration time, the remaining headspace was analysed for CO₂ concentrations using a gas chromatograph (see Section
below), and total dissolved concentrations were calculated based on Henry's law (see a detailed method in Supplementary).

190 For each date, pCO_{2w} samples were taken in triplicate with an average coefficient of variation (CV) of 8%.

2.3 Gas Chromatography

Gas samples were analysed at ETH Zurich using a gas chromatograph (GC3-Bruker, 456-GC, Scion Instruments, Livingston,
UK) separating CO₂ from residual air. After separation, the concentration of CO₂ was measured on a thermal conductivity
detector. GC calibration was done with a suite of three standards (Carbagas AG, Switzerland; PanGas AG, Switzerland) across
195 a concentration range from 249 to 3040 ppm CO₂. Each standard was analysed ten times at start, middle, and end of each set
of 140-180 samples. Moreover, because of occasional high CO₂ sample concentrations, an entire system flush was done
between each sample measurement to avoid any carry-over effects. The same GC setup was used for both flux samples and
dissolved CO₂ samples.

2.4 $\delta^{13}C$ of soil-derived CO₂ fluxes and dissolved CO₂

200 The carbon isotopic composition of the CO₂ samples was analysed for one SFF CO₂ flux sample set of each month. That is,
after CO₂ concentration measurement with the GC, the same samples were analysed for $\delta^{13}C$ of CO₂ with a modified Gasbench
II periphery (Finnigan MAT, Bremen, D) coupled to an isotope ratio mass spectrometer (IRMS; Delta^{plus}XP; Finnigan MAT)
as described in Baumgartner et al. (2020). Post-run off-line calculation and drift correction for assigning the final $\delta^{13}C$ values
on the Vienna Pee Dee Belemnite (V-PDB) scale was done following the “IT principle” (R. A. Werner and Brand 2001). The
205 $\delta^{13}C$ -values of the laboratory air standards were determined at the Max-Planck-Institute for Biogeochemistry (Jena, Germany),

according to Werner, Rothe, and Brand (2001). The final soil CO₂-δ¹³C values were calculated using the Keeling plot approach (Keeling 1958) (Supp. Fig. 2).

δ¹³C of dissolved riverine CO₂ was determined using the headspace equilibration technique as described in section 2.2.2.

210 Instead of concentration, δ¹³C of the headspace was analysed via IRMS as described above. Samples were taken each month from the Ruki river between 10-2022 to 06-2023 with 2-3 replicates per sampling (Supp. Fig. 4).

2.5 δ¹³C of leaves, litter, and soils

Fresh leaf samples were taken from a range of the most representative tree species at two different timepoints (2019-11; 2023-11). In addition, litter samples were collected at the same time and both were used to analyze the carbon isotopic composition
215 (δ¹³C). Before analysis samples were dried, homogenized, and ground. Soil samples were taken in 2019-11, 2020-02 and 2023-11 at 0-30 cm depth and air dried, sieved, and milled. All samples were analyzed using an elemental analyzer (Flash EA 1112 Series, Thermo Italy, former CE Instruments, Rhodano, Italy), interfaced with an IRMS (Finnigan MAT Delta^{plus}XP, Bremen, Germany) via a 6-port valve (Brooks et al. 2003) and a ConFlo III (Werner et al. 1999). Soil samples are subsequently referred to as soil organic carbon (SOC) samples. Calibration of laboratory standards (acetanilide, caffeine, tyrosine) was done by
220 comparison to the corresponding international reference materials provided by the IAEA (Vienna, Austria).

2.6 Water ~~level~~table

Direct measurements of the water ~~table-level~~ were not available for the whole observation period. Previous work showed a linear relationship between the water level of the Congo River and the Ruki river (unpublished, Supp. Fig. 3). Additionally, the rainfall and/or the hydrological dynamics of the river influence the water levels in the wetlands. In the *Cuvette Centrale*,
225 Georgiou et al. (2023) ~~showed-determined~~ that the water levels of riverine locations in the Democratic Republic of ~~the~~ Congo (DRC) correlate more with the hydrological dynamics of the river system than with the rainfall input. Hence, available daily measurements of the water level of the Congo River in Mbandaka were used as a proxy of the water ~~table-level below- and aboveground at the SFF site~~. (Supp. Fig. 6). This data was extracted from an almost continuous record of water gauge readings, collected ~~in vicinity of the SFF site (~ 4 km)~~-by the Congolese public institution, *Régie des Voies Fluviales*, since 1913.

230 2.7 Statistical Analyses

Daily environmental conditions were used to explain variability in the measured soil CO₂ fluxes (n = 403) at the SFF site. For this, a linear mixed effects model was fitted using soil temperature, volumetric soil water content, and river level as fixed effects. River level showed a non-linear relationship with surface fluxes. Hence, a quadratic term was added to account for the non-linear effect. The predictor variables were standardized before fitting the models. All models controlled for repeated
235 measurements in the same chambers, by adding chamber ID as a random intercept. Models were fitted by the restricted

maximum likelihood method using *lme4* (Bates et al. 2015). Full and reduced models were compared using likelihood ratio test and adjusted R^2 values using *MuMin* package (Barton 2020). Furthermore, a backward stepwise regression analysis was conducted on the full model, incorporating all effects and interaction terms, to identify the most parsimonious model with highest explanatory power (Kuznetsova et al., 2017). The resulting model included an additional interaction term between soil moisture and river level. However, this term was subsequently removed due to multicollinearity and its lack of practical significance. Marginal and conditional R^2 values for mixed effects were calculated using Nakagawa, ~~Johnson, and Schielzeth~~ et al., (2017), ~~inclusive R^2 estimated with partR2 package (Stoffel et al., Nakagawa, and Schielzeth 2021)~~, and p-values ~~were estimated~~ using Satterthwaite's approximation ~~using with the lmerTest package (Kuznetsova et al., 2017)~~. Additionally, confidence intervals for the effect estimates were computed to confirm the interpretation of the estimated parameters. The assumptions of the model were validated by verifying the linearity, normality and homoscedasticity of the residuals. Multicollinearity between the predictor variables was also estimated (Variance Inflation Factor (VIF) inferior to 3). ~~Statistical differences between $\delta^{13}\text{C}$ values measured across the different carbon pools were tested with the Kruskal-Wallis test, followed by a pairwise Wilcoxon comparisons. Significance was established when the Bonferroni adjusted p-values were inferior to 0.05.~~ Statistical and graphical data analysis was done in R v.4.3.2 (R Core Team 2023) via RStudio v.2023.12.0 (RStudio Team 2023), using the packages *tidyverse* v.2.0.0, *tydr* v.1.3.0, *dplyr* v.1.1.4 (Wickham et al. 2023), *ggplot2* v. 3.4.4 (Wickham 2009), *sjPlot* (Lüdtke 2013) and *lubridate* v.1.9.3 (Grolemund and Wickham 2011). QGIS version 3.16 was used to compile the map of the sampling locations.

3 Results

3.1 Precipitation, soil moisture, and temperature ~~Environmental Conditions~~

The long dry season in Mbandaka is considered from July to August whereas the short dry season spans between January and February. However, frequent rainfall as shown in Figure 3 ~~Figure-3~~ renders the region as relatively wet throughout the entire year. Annual precipitation was the highest in 2020 with 1855 mm and lowest in 2022 with 1417 mm (self-measured; Figure 3 ~~Figure-3~~). The flooding period at the study site is typically centered around December and January. ~~Annual precipitation was the highest in 2020 with 1855 mm and lowest in 2022 with 1417 mm.~~ The highest weekly precipitation occurred in July and September of each year with 120 – 182 mm (Figure 3 ~~Figure-3~~ A). Overall, the weekly precipitation ranged from 0 – 182 mm, with a monthly average of 31 mm (Figure 3 ~~Figure-3~~ A).

Volumetric soil water content averaged $0.60 \pm 0.09 \text{ m}^3 \text{ m}^{-3}$, ranging between 0.35 to $0.76 \text{ m}^3 \text{ m}^{-3}$ for the observation period (Figure 2A). In general, the soil moisture showed strong seasonality, with an increase in November and peak values observed in January. Thereafter, the soil moisture decreased before stabilizing until the following wet season. This pattern was less pronounced over the 2021-2022 season (Figure 3 ~~Figure-3~~ A).

Soil and air temperatures were stable throughout the observation period (Figure 3B). Recorded mean air temperature at the weather station was 25.0 °C (± 0.7 °C), and mean soil temperature at the SFF site was 24.7 °C (± 0.3°C) for the observation period.

3.2 Soil and aquatic CO₂ fluxes

Over the observation period, CO₂ fluxes from the PFF site were higher than from the SFF site (Figure 3C). At both sites, CO₂ fluxes exhibited intra-annual variability. However, distinct seasonal patterns were not clear. Notably, at the SFF site, the onset of flooding appeared to induce a decline in fluxes. Furthermore, among the environmental variables, CO₂ fluxes exhibited significant correlations with soil moisture, soil temperature, and river level (Table 1). At the PFF site, the highest fluxes were recorded in June and August of 2020 with 5.71 and 5.76 μmol m⁻² s⁻¹, whereas the lowest values were observed in September and October 2020 with 3.35 and 3.42 μmol m⁻² s⁻¹. Mean weekly surface fluxes (F_{CO2}) from the PFF site ranged from 3.35 to 5.76 μmol m⁻² s⁻¹ with an average flux of 4.38 ± 0.64 μmol m⁻² s⁻¹ using the *in-situ* derived gas transfer velocity of 3.5 cm h⁻¹ (Figure 3C). Mean weekly surface fluxes (F_{CO2}) from the SFF site ranged from 0.87 to 3.64 μmol m⁻² s⁻¹ with an average of 2.36 ± 0.51 μmol m⁻² s⁻¹. Here, the lowest flux was observed in July 2022 with 0.87 μmol m⁻² s⁻¹, period corresponding to the lowest soil moisture recorded (0.35 m³ m⁻³), while peaking in May 2020 with 3.64 μmol m⁻² s⁻¹ (Figure 3C).

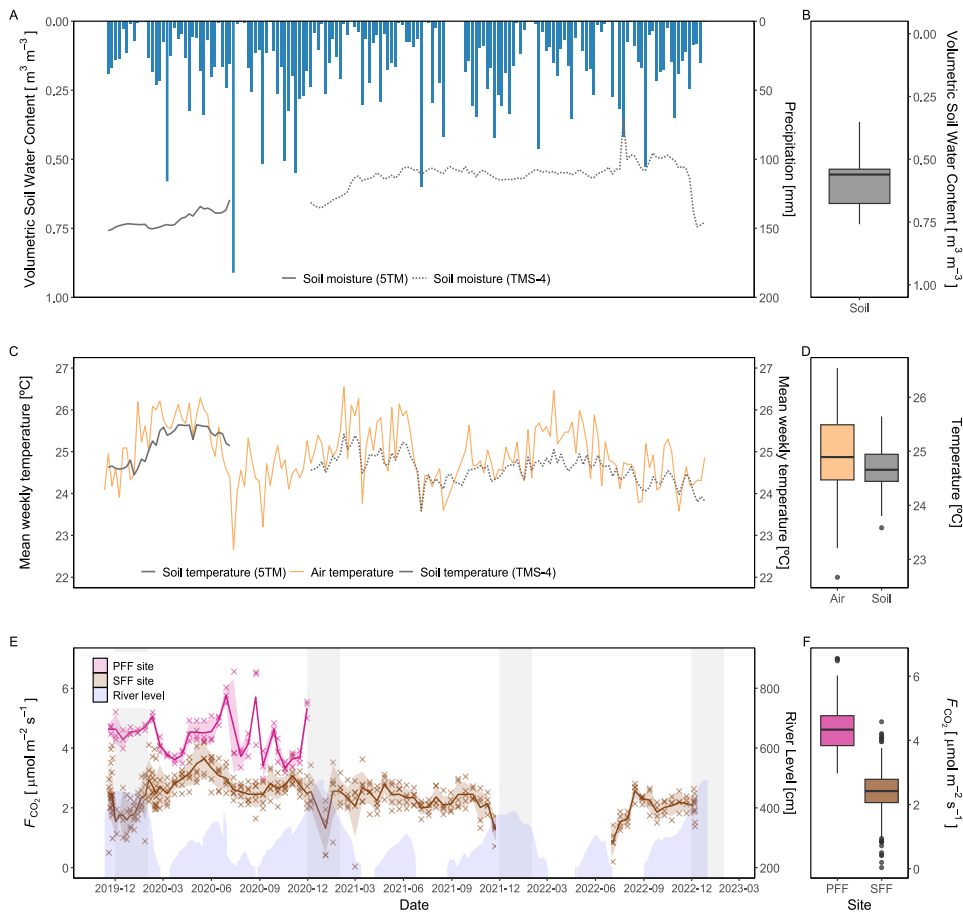


Figure 3. Weekly precipitation, volumetric soil water content, temperature, and CO_2 fluxes. (A) The sum of the weekly precipitation [mm] (blue) obtained from the Trans-African Hydro-Meteorological Monitoring Observatory and mean volumetric soil water content [$\text{m}^3 \text{m}^{-3}$] measured with soil moisture sensors (ECH2O 5TM = solid line, TMS-4 dataloggers = dotted line). (B) Distribution of volumetric soil water content [$\text{m}^3 \text{m}^{-3}$], both sensor types combined. (C) Mean weekly air temperature [$^{\circ}\text{C}$] (gold) was obtained from the Trans-African Hydro-Meteorological Monitoring Observatory. The mean weekly soil temperature [$^{\circ}\text{C}$] was measured with soil temperature sensors (ECH2O 5TM = grey solid line, TMS-4 dataloggers = grey dotted line). (D) Distribution of air and soil temperatures [$^{\circ}\text{C}$], both sensor types combined. (E) Calculated mean weekly measured surface CO_2 fluxes (crosses) [$\mu\text{mol m}^{-2} \text{s}^{-1}$] from the SSF site (brown) and calculated CO_2 fluxes from the PFF site with a calculated-K of 3.5 cm h^{-1} (pink). All measurements (linecross) and the standard error of the mean are displayed. Blue shading

295

300

305

310

315

Formatted: Font color: Auto

320 R^2 (IR^2) of each predictor is also presented, offering a measure of the proportion of variance explained by each predictor, including both its direct effects and interactions with other predictors (Stoffel et al., Nakagawa, and Schielzeth 2021). In this context, the soil temperature ($IR^2 = 0.225$), soil moisture ($IR^2 = 0.126$), and the quadratic component of the river level ($IR^2 = 0.097$) appear as the primary factors explaining the variance of surface CO_2 fluxes, whereas the interaction between soil temperature and river level ($IR^2 < 0.001$), along with the linear component of the river level ($IR^2 = 0.001$), make no meaningful contribution (Figure 4). Figure 4. Individual relationships between soil CO_2 fluxes and the environmental parameters (volumetric soil water content (VWC) (A), soil temperature (B) and river level (C)). Measures taken while the soil chamber was partially flooded are represented in green. Regression lines are displayed in brown. The interaction between soil temperature and river level is illustrated (D). Values were predicted based on the LMER model (Table 1).

325

- Formatted: Font color: Auto
- Formatted: Font color: Auto
- Formatted: Font color: Auto
- Formatted: Font color: Auto
- Formatted: Font color: Auto, Not Highlight
- Formatted: Font color: Auto
- Formatted: Font color: Auto
- Formatted: Font color: Auto
- Formatted: Font color: Auto, Not Highlight
- Formatted: Font color: Auto
- Formatted: Font color: Auto, Not Highlight
- Formatted: Font color: Auto
- Formatted: Font color: Auto

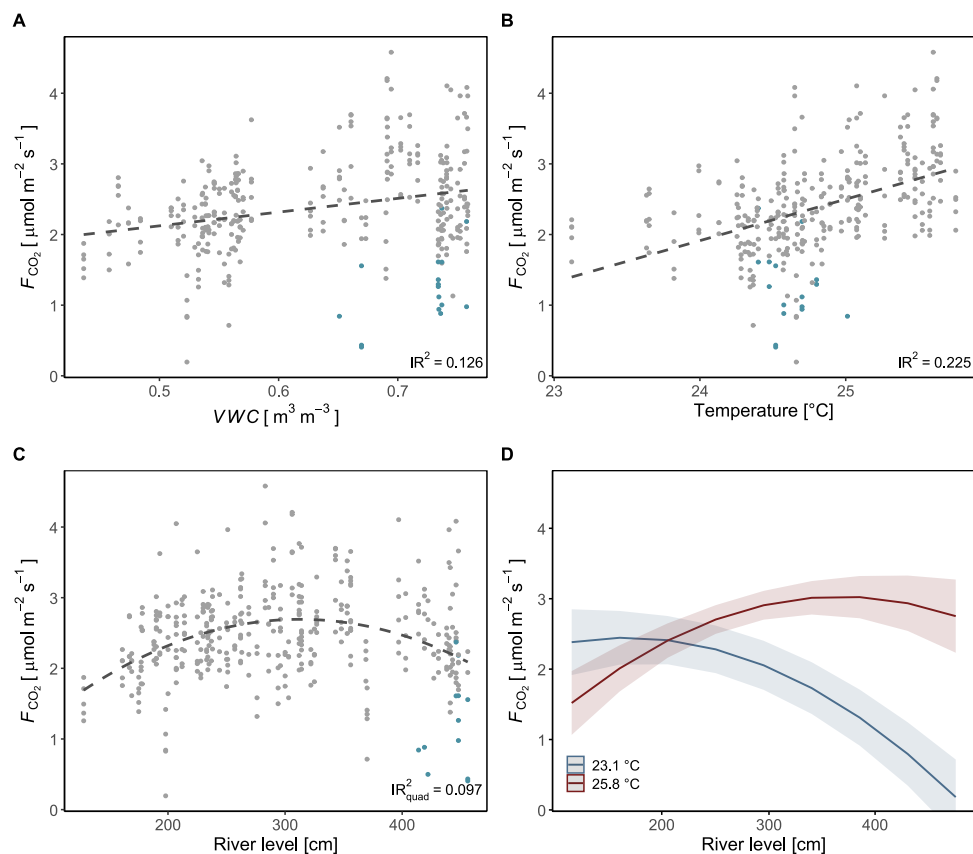


Figure 4. Individual relationships between soil CO₂ fluxes and the environmental parameters (volumetric soil water content (VWC) (A), soil temperature (B), and river level (C)). Measures taken while the soil chamber was partially flooded are represented in green. Regression lines are displayed as dashed black lines. The interaction between soil temperature and river level is illustrated. Values were predicted based on the LMER model (Table 1) (D). Inclusive R^2 (A, B, C) was estimated based on the LMER model (Table 1; Stoffel et al., 2021). Individual relationships between soil CO₂ fluxes and the environmental parameters (volumetric soil water content (VWC) (A), soil temperature (B) and river level (C)). Measures taken while the soil chamber was partially flooded are represented in green. Regression lines are displayed in brown. The interaction between soil temperature and river level is illustrated. Values were predicted based on the LMER model (D). Values were predicted based on the LMER model (Table 1). (Stoffel, Nakagawa, and Schielzeth 2021)

Formatted: Font color: Auto

Formatted: Font color: Auto

Formatted: Font color: Auto

Formatted: Font color: Auto

Formatted: Font color: Auto

Formatted: Font color: Auto

Formatted: Font color: Auto

3.2.2. Controls on surface CO₂ fluxes at the PFF site

At the PFF site, surface CO₂ fluxes ~~did not exhibit statistically significant relationships with pH, river level, carbon to nitrogen ratio (C:N), dissolved organic carbon, or biodegradable dissolved organic carbon. Trends were observed, such as an increase in CO₂ fluxes with rising river levels and opposing trends with pH. CO₂ fluxes appeared to decrease as pH increased. However, these are just visual tendencies and not statistically significant.~~
~~a slight increase with the river level, while pH demonstrated opposing trends. Following this pattern, the aquatic CO₂ fluxes decreased with pH increase. It is important to note, however, that these observations reflect visual trends rather than statistically significant findings.~~
~~exhibited a slight increase with the river level, while pH demonstrated opposing trends. Following this pattern, the aquatic CO₂ fluxes decreased with pH increase. It is important to note, however, that these observations reflect visual trends rather than statistically significant findings. No relationship between the carbon to nitrogen ratio (C:N), dissolved organic carbon or biodegradable dissolved organic carbon and CO₂ fluxes was observed.~~

Formatted: Font color: Auto

3.3 $\delta^{13}\text{C}$ of leaves, litter, soils, soil CO₂ flux, and riverine dissolved CO₂

The measured $\delta^{13}\text{C}$ values increased from leaves over litter and SOC to soil CO₂ fluxes and became more positive along this cascade of organic matter transformation (~~p-values < 0.05; Figure 5~~Figure-5). $\delta^{13}\text{C}$ of leaves ranged from -37.1 to -28.9‰ with a mean of $-33.8 \pm 2.1\text{‰}$. The $\delta^{13}\text{C}$ signature of litter was between -32.6 and -28.7‰ and, on average $-30.5 \pm 1.0\text{‰}$. SOC had $\delta^{13}\text{C}$ of -30.1 to -22.3‰, while the mean was $-27.4 \pm 1.9\text{‰}$. The $\delta^{13}\text{C}$ of soil-derived CO₂ (F_{CO2}) was in the range of SOC values for the SFF site (~~Figure 5~~Figure-5) and very stable throughout the measurement period (Supp. Fig. 4). Here, measured $\delta^{13}\text{C}$ values were -30.2 to -26.5‰ with a mean of $-28.5 \pm 0.8\text{‰}$. Contrary, the carbon isotopic composition of CO₂ fluxes from the SFF site during flooding was strongly ¹³C enriched with -24.8 to -13.3‰ and an average of $-20.4 \pm 3.4\text{‰}$ (~~p-values < 0.01~~). The $\delta^{13}\text{C}$ of the inundated soil CO₂ fluxes was higher throughout the whole measurement period (Supp. Fig. 4). The $\delta^{13}\text{C}$ value of dissolved CO₂ from the adjacent Ruki river was highly stable throughout the measurement period from 2022-10 to 2023-06 ranging from -24.9 to -23.3‰ with a mean of $-24.3 \pm 0.5\text{‰}$ (Supp. Fig. 4).

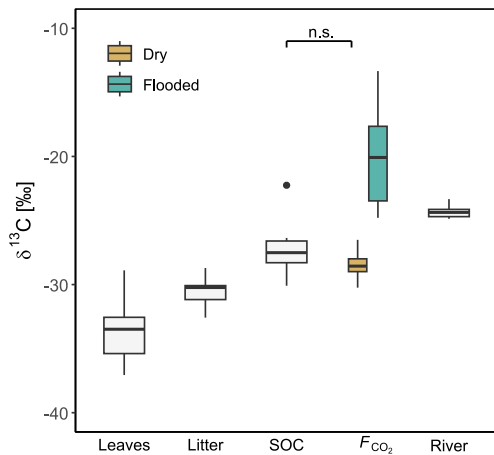


Figure 5. $\delta^{13}\text{C}$ values of leaves, litter, soil organic carbon (SOC), soil CO_2 flux (F) at the SFF site as well as riverine dissolved CO_2 (Ruki river). Surface CO_2 flux (F) is further separated into dry and inundated based on chamber type (floating, static). Non-significant difference between SOC and dry F_{CO_2} is indicated by n.s.

4 Discussion

4.1 CO_2 fluxes

The surface CO_2 flux dataset from the SFF site, measured for three consecutive years, showed intra-seasonal and interannual variability. However, no clear seasonal patterns were observed (Figure 3E). Baumgartner et al. (2020) showed a similar low seasonality in lowland forests of the Congo Basin, attributing it to the limited rainfall variation between dry and wet seasons. The unclear seasonal pattern of the CO_2 fluxes at the SFF site could be attributed to the lasting effect of the flooding (Docherty and Thomas 2021) and/or consistent rain events during the whole year (Figure 3A-B). These factors, along with the brief duration of both dry seasons, may lead to soil moisture contents remaining near optimal conditions for vegetation and soil microbes to thrive. Such uniform environmental conditions may maintain autotrophic and heterotrophic respiration at a steady level despite undergoing a discernible dry and wet season cycle. Baumgartner, et al. (2020) (Docherty and Thomas 2021) The reported mean flux of $2.36 \pm 0.51 \mu\text{mol m}^{-2} \text{s}^{-1}$ from the SFF site was lower compared to previous studies in

the Congo Basin. These studies found mean values of respectively $3.13 \pm 1.22 \mu\text{mol m}^{-2} \text{s}^{-1}$, $3.45 \pm 1.14 \mu\text{mol m}^{-2} \text{s}^{-1}$ in
montane and lowland forests (Baumgartner et al. 2020) and $4.07 \pm 0.90 \mu\text{mol m}^{-2} \text{s}^{-1}$ in a lowland secondary forest of Cameroon
bordering the Congo Basin (Verchot et al. 2020). Compared to similar tropical forest studies, our values are at the low end of
the range reported across the pantropical forest realm (Table 2).

The perennially flooded forest site (PFF), located at the interface between terrestrial (forest) and aquatic (stream) ecosystems
showed relatively high emissions ($4.38 \pm 0.64 \mu\text{mol m}^{-2} \text{s}^{-1}$) when compared to other tropical flooded forests (Scofield et al.
2016; Table 2). ~~tropical forests~~ or to those streams draining catchments dominated by seasonally or continually inundated
swamp forests (Mann et al., 2014; Alin et al. 2011; Table 2). The elevated CO₂ fluxes at the PFF site resulted in higher fluxes
relative to the SFF site. Further research is needed to determine whether a greater water depth-integrated respiration (Amaral
et al. 2020), a positive correlation with a larger inundated area (Amaral et al. 2020), prolonged river interactions or other
factors explain such difference. In contrast, the SFF site presented reduced CO₂ fluxes during the onset of flooding,
speculatively due to the inhibitory effect of excessive soil moisture on soil respiration (Courtois et al. 2018; Nissan et al. 2023).
A non-significant positive trend between water level and the aquatic CO₂ fluxes was visually discernible which is in line with
a positive relationship between pCO₂ and discharge measured on the adjacent Ruki (Drake et al., 2023). As a constant gas
transfer velocity was used in the present study, short-term changes in aquatic CO₂ fluxes reflect the variations in carbon dioxide
concentrations (pCO₂) in the water. Similarly, Drake et al. (2023) reported a positive relationship between pCO₂ and discharge
on the adjacent Ruki. Moreover, the generally low gas transfer velocity (3.5 cm h^{-1}) reflects further the very
high pCO₂ concentrations ($10197 - 17260 \text{ ppm}$) measured at the PFF site. These values are significantly higher than the range
($3069 - 9088 \text{ ppm}$) found by on the adjacent Ruki river (Drake et al. (2023). However, the adjacent Ruki water has a long
transit time compared to a swamp and a stronger current which in turn results in higher CO₂ outgassing. Generally, the pCO₂
concentration itself is driven by factors such as terrestrial inputs, gas exchange with the atmosphere, water temperature (gas
solubility), water chemistry (pH, alkalinity), and in-stream metabolism (Rocher-Ros et al. 2019; Hotchkiss et al. 2015; Battin
et al. 2023). (Amaral et al. 2020)

Finally, the *in-situ* derived gas transfer velocity (k_a) expressed as normalized k_{600} (2.95 cm h^{-1}) was ~~slightly~~ higher than the
global normalized estimate (k_{600}) for tropical wetlands (2.4 cm h^{-1} ; Aufdenkampe et al. 2011). The gas transfer velocity itself
changes by factors influencing the near-surface water turbulence (wind speed, water current velocity). ~~A non-significant
positive relationship between water level and pCO₂ was found (Figure 5).~~ Generally, assuming a constant gas transfer velocity
(k_a), as applied in this study, has its limitations since it likely varies throughout the year with increased values during the dry
season when the water is flowing in the stream bed channel (Alin et al. 2011).

Table 2. Reported mean values of surface CO₂ fluxes across various tropical forested environments

Country/Basin	Environment	Temporal coverage	Fco ₂ (μmol m ⁻² s ⁻¹)	Source
DRC / Congo Basin	Seasonally flooded forest	3 years	2.36 ± 0.51	This study
	Perennially flooded forest	1 year	4.38 ± 0.64	
DRC / Congo Basin	Montane and lowland (<i>terra firme</i> ¹) forests	3 years, at varying temporal resolution	3.13 to 3.45	Baumgartner et al. (2020)
DRC / Congo Basin	Lowland (<i>terra firme</i> ¹) forest	16 months, sub-daily resolution	4.04 ± 1.16	Daelman et al. (2024)
ROC / Congo Basin	Streams (< 100 m wide) draining swamp forests	3 punctual campaigns over the hydrological year	3.61 ± 1.46	Mann, Spencer, et al. (2014)
Cameroon	Lowland (<i>terra firme</i> ¹) forest	17 months	4.07 ± 0.90	Verchot et al. (2020)
Kenya	Montane (<i>terra firme</i> ¹) forest	2-3 months, dry season and transition period	1.04 to 1.66	Arias-Navarro et al. (2017); Werner, Kiese, and Butterbach-Bahl (2007)
Panama	Lowland poorly drained forest	3 years	4.26 ± 0.16	Rubio and Detto (2017)
Brazil / Amazonian Basin	Seasonally flooded forest	From 1 to 2 years, at varying temporal resolution	2.2 ² t 5.28	Amaral et al. (2020); Borges Pinto et al. (2018); Zanchi et al.(2011)
Brazil / Rio Negro Basin	Perennially flooded forest	Punctual campaigns (low and high-water periods)	0.52 ± 0.21	Scofield et al. (2016)
Brazil / Amazonian Basin	Streams (< 100m wide) draining Amazonian wetlands	Punctual field campaigns integrating low and high flow periods	5.45 ± 3.39 to 5.49 ± 3.16	Alin et al. (2011); Rasera et al. (2008)
Amazonian Basin	Lowland (<i>terra firme</i> ¹) forest	Variable	2.30 to 5.30	(Davidson, Ishida, and Nepstad (2004); Doff sotta et al. (2004); Sousa Neto et al. (2011); Sotta et al. (2007); Garcia-Montiel et al. (2004); Borges Pinto et al. (2018); Janssens, Tête Barigah, and Ceulemans (1998); Buchmann et al. (1997); Bréchet et al. (2021); Epron et al. (2013); Courtois et al. (2018);
Thailand	Lowland (<i>terra firme</i> ¹) forest	Punctual measurements over 2.5 years	6.57 ± 3.42 ³	Adachi et al. (2009)

Malaysia	Lowland (<i>terra firme</i> ¹) forest	Punctual measurements over 2 and 4 years	5.32 ± 2.85 to 5.7 ± 1.9	Katayama et al. (2009); Ohashi et al. (2007)
Australia	Seasonally flooded forest	13 months	1.4 ± 1.0 / 2.4 ± 1.4 (dry season / wet season)	Goodrick et al. (2016)

¹ Terra firme forests refer here to non-flooding forests.

² Measurements done only during the inundated period

³ -Mean soil respiration for the wet season

4.2 Temperature, soil moisture and water ~~table-depth~~level controls

While the observed CO₂ fluxes at the SFF site showed no clear seasonal pattern, soil temperature, soil moisture and the river level as proxy of the water ~~table-level~~ emerged as significant controls. While the positive effect of temperature and soil moisture on soil CO₂ fluxes is well known and used to model soil CO₂ fluxes (Nissan et al. 2023), the effect of water ~~table-level~~ is less well understood. The observed quadratic relationship with ~~the water table-depth~~level suggests an optimal water level beyond which further increases lead to reduced CO₂ fluxes. This optimal point likely corresponds to the shift to water saturated conditions in the organic-rich surface soil transitioning from oxic to anoxic conditions. A negative effect of ~~the water table-level~~ beyond a critical threshold aligns well with the results of Goodrick et al., (2016). That study found maximal soil CO₂ fluxes associated with a ~~table-depthwater level~~ between 1.5 and 2 m below ground and minimal fluxes when the water ~~table-level~~ was within 0.15 m of the surface for a tropical riparian swamp forests in Australia (Goodrick et al. 2016). Similarly, Rubio and Detto (2017) found a quadratic relationship between CO₂ fluxes and soil water content in the Amazonian basin. CO₂ fluxes can be reduced in both high and low soil water content, and fluctuations in water ~~table-depth~~level introduce additional factors beyond its influence on soil saturation. Both heterotrophic and autotrophic soil respiration are reduced under dry conditions due to limited microbial activity and reduced photosynthetic activity through stomatal closure (Baumgartner et al. 2020). In our study, the lowest flux event recorded in July 2022 coincided with a marked decrease in soil moisture. This suggests that, during this event, the reduced soil moisture levels became a limiting factor for supporting soil respiration. Conversely, increased soil moisture generally enhances respiration. This was generally the case during our study period, as evidenced by the positive correlation between soil moisture and surface CO₂ fluxes (p-value < 0.05; Table 1). However, excessively high moisture conditions (due to strong rain events or high water ~~tables~~level during flooding) can also hinder substrate decomposition by physically impeding the diffusion of atmospheric oxygen and respired CO₂ through the soil pores, thereby limiting both the production and diffusion of CO₂ (Courtois et al. 2018; Nissan et al. 2023). This could explain the temporary decrease in CO₂ fluxes observed at the onset of the flooding period (Figure 3Figure-3). Furthermore, fluctuations in the water ~~table-depth~~level can influence soil respiration through physical processes like flushing out soil CO₂ during rising phases, enhanced lateral movement of dissolved CO₂, as well as air ingress and redistribution of organic material during

receding phases (Goodrick et al. 2016; Dalmagro et al. 2018). Finally, the positive interaction between soil temperature and water ~~table~~_{level} ($p\text{-value} < 0.05$; Table 1) suggests that higher temperatures will reinforce the effect of the water level and shift the maximum soil flux towards higher ~~levels of the water table~~_{water levels} delaying its inhibitive effect (Figure 4Figure 4).

Nevertheless, it is important to note that both the water ~~table~~_{level} and soil moisture measurements exhibit seasonal patterns but do not capture well the short-term changes of the ~~surface~~_{soil} CO₂ fluxes ~~at SFF site~~. Furthermore, the CO₂ fluxes exhibit unclear seasonal pattern (Supp. Fig. 5B). ~~This suggests that other factors, such as aboveground inputs from vegetation, river sediment deposition, and rain-induced events, may significantly influence surface~~_{soil} CO₂ fluxes, both in the short term and at ~~seasonal~~_{over longer} timescales. Additionally, it is important to stress that using ~~the river level as a proxy for the water table~~_{level at the SFF site} presents limitations such as neglecting local topography or soil characteristics. ~~Thus, fortnightly variations in soil CO₂ fluxes may not be fully captured by this proxy, as local hydrological dynamics might differ from those of the broader river system. Hence, this method may not fully capture the dynamics of the water table~~_{level and its influence on surface}_{soil} CO₂ fluxes.

~~This suggests that other factors, such as aboveground inputs, deposition, and rain-induced events, may significantly influence soil CO₂ fluxes, both in the short term and over longer timescales.~~ Overall, while soil ~~water~~_{moisture} content and temperature are often considered primary drivers of soil CO₂ fluxes (Courtois et al. 2018; Oertel et al. 2016; Nissan et al. 2023), our findings also indicate that incorporating water ~~table~~_{depth}_{level} can help to unravel the variability of the fluxes for lowland forests with shallow water tables.

At the PFF site, on the other hand, we did not find any statistically significant relationships between potential drivers (DOC, BDOC, ~~river~~_{water} ~~table~~_{level}, pH, C:N) and $p\text{CO}_{2w}$. This suggests that the chemical composition of the water is relatively homogenous throughout the year and that allochthonous rather than autochthonous processes determine $p\text{CO}_{2w}$ concentrations.

4.3 Isotopic indicators

The general carbon isotopic composition of plant tissue is determined by the degree of ¹³C discrimination at the leaf level (Brüggemann et al., 2011). Due to the high photosynthetic activity of tropical plants, ¹³C discrimination is also high, resulting in very negative $\delta^{13}\text{C}$ values at the leaf level as observed in this study (-37.06 to -28.89‰). As the C moves across the various ecosystems C pools, the substrate becomes gradually enriched in ¹³C due to kinetic isotope fractionation. In the case of the studied SFF site, a total ¹³C enrichment of 5.27‰ was observed when moving down the cascade from leaves, litter, SOC to respired CO₂ under dry conditions ($p\text{-values} < 0.05$; Figure 5Figure-5). Particularly interesting here is the absence of ¹³C fractionation between SOC and soil respired CO₂, which might initially be interpreted as a result of closed system dynamics where the substrate is limited, and organic decomposition tends to be complete. However, soil respired CO₂ is a two-component flux, comprised of heterotrophic and autotrophic respiration. In other words, SOC is not the sole factor governing soil respired

CO₂. Indeed, autotrophic respiration is to a large degree fueled by recently photosynthesized ¹³C depleted C (Högberg et al., 2001, Barthel et al., 2011) which in turn can decrease the overall soil respired δ¹³C value relative to SOC (depending on the relative contribution of autotrophic vs heterotrophic soil respiration). Transport rates from above to belowground can reach up to 0.5 m h⁻¹ (Kuzakov and Gavrichkova 2010). Thus, whether the similar δ¹³C values between SOC and respired CO₂ are driven by substrate limitation or a strong influence of autotrophic respiration requires further investigation.

The highest ¹³C enrichment observed was from CO₂ emitted during flooding at the SFF site (~~-20.4‰~~;-20.4‰; p-values < 0.05). These δ¹³C values were even higher than the δ¹³C values measured in the adjacent Ruki river (~~-24.30 ‰~~; p-value < 0.05;-24.30 ‰). The reason for such highly ¹³C enriched CO₂ outgassing during inundation remains unclear but given that the water in the inundated forest likely experiences relatively long residence times compared to the river, the outgassed CO₂ might become this heavily ¹³C-enriched due to extensive outgassing. Moreover, the standing water allows the growth of methanogenic archaea which use simple carbon compounds such as acetate as electron donors (Conrad et al., 2021). The CO₂ molecules obtained from acetate cleavage is another fractionation process which potentially influences the overall isotopic composition of outgassed CO₂. Lastly, as the inundation of the SFF site is mainly driven by backflow from the river system, the dissolved CO₂ in the inundated water could be a mix of riverine and locally soil-respired CO₂ that undergoes further *in-situ* ¹³C enrichment.

5 Conclusion

This study presents a multi-year dataset of CO₂ fluxes from two forested wetland sites along a flooding gradient : a seasonally flooded forest (SFF) and a perennially flooded forest (PFF). While exhibiting short-term and interannual fluctuations, CO₂ fluxes showed limited seasonal patterns. At the SFF site, surface emissions increased with rising soil moisture and temperature, while the water ~~table~~-level demonstrated a significant quadratic relationship. Despite the significant sensitivity to environmental conditions over the observation period, the short-term variability observed at both sites, as well as the interannual variability at the SFF site, were incompletely explained, suggesting the influence of additional factors in regulating emissions.

Our results emphasize that ~~ground~~water level, alongside soil temperature and soil moisture, significantly affects surface CO₂ fluxes in lowland areas with shallow, fluctuating water tables. Future research should include direct measurements of the water ~~table-level~~ over the entire hydrological year to elucidate the temporal dynamics of this relationship. Overall, the reported measurements contribute to filling the data gap for soil respiration rates of tropical forests in the Congo Basin and provide baseline fluxes for parametrizing earth system models.

Data Availability

All data used in this study will be made available through the soil respiration database (SRDB; Jian, J. et al. 2021).

Author contributions

505 Mbarthel, MBauters, TWD, KVO, and JS were responsible for study design and conceived the study. Fieldwork was conducted by Mbarthel, MBauters, TWD, SB, NBM, JC, ADC, and CE. Lab work was conducted by Mbarthel, RAW, SB and JC. Data analyzes and interpretation was performed by ACHJ, ADC, MBauters and Mbarthel. ADC and ACHJ wrote the manuscript with contributions from all co-authors.

Competing Interests

510 At least one of the (co-)authors is a member of the editorial board of Biogeosciences.

Acknowledgements

The authors would like to thank the Trans-African Hydro-Meteorological Monitoring Observatory (TAHMO) for providing meteorological data from the investigated site and the ICCN park guards for assistance in the field. The authors would like to further thank Annika Ackermann from the Grassland Science group (Prof. Buchmann) at ETH Zurich for the stable isotope analysis of plant and soil materials.

Funding Statement

The core funding of ETH Zurich financed this study. MBarthel received funding from the Swiss National Science Foundation (IZSEZ0_186376 / 1).

520 **References**

Adachi, Minaco, Atsushi Ishida, Sarayudh Bunyavejchewin, Toshinori Okuda, and Hiroshi Koizumi. 2009. "Spatial and Temporal Variation in Soil Respiration in a Seasonally Dry Tropical Forest, Thailand." *Journal of Tropical Ecology* 25 (5): 531–39. <https://doi.org/10.1017/S026646740999006X>.

525 Alin, Simone R., Maria de Fátima F. L. Rasera, Cleber I. Salimon, Jeffrey E. Richey, Gordon W. Holtgrieve, Alex V. Krusche, and Anond Snidvongs. 2011. "Physical Controls on Carbon Dioxide Transfer Velocity and Flux in Low-Gradient River Systems and Implications for Regional Carbon Budgets." *Journal of Geophysical Research: Biogeosciences* 116 (G1). <https://doi.org/10.1029/2010JG001398>.

- Alsdorf, Douglas, Ed Beighley, Alain Laraque, Hyongki Lee, Raphael Tshimanga, Fiachra O'Loughlin, Gil Mahé, Bienvenu Dinga, Guy Moukandi, and Robert G.M. Spencer. 2016. "Opportunities for Hydrologic Research in the Congo Basin." *Reviews of Geophysics* 54 (2): 378–409. <https://doi.org/10.1002/2016RG000517>.
- Amaral, Joao Henrique Fernandes, John M. Melack, Pedro Maia Barbosa, Sally MacIntyre, Daniele Kasper, Alicia Cortés, Thiago Sanna Freire Silva, Rodrigo Nunes de Sousa, and Bruce R. Forsberg. 2020. "Carbon Dioxide Fluxes to the Atmosphere From Waters Within Flooded Forests in the Amazon Basin." *Journal of Geophysical Research: Biogeosciences* 125 (3): e2019JG005293. <https://doi.org/10.1029/2019JG005293>.
- Arias-Navarro, C., E. Díaz-Pinés, S. Klatt, P. Brandt, M. C. Rufino, K. Butterbach-Bahl, and L. V. Verchot. 2017. "Spatial Variability of Soil N₂O and CO₂ Fluxes in Different Topographic Positions in a Tropical Montane Forest in Kenya." *Journal of Geophysical Research: Biogeosciences* 122 (3): 514–27. <https://doi.org/10.1002/2016JG003667>.
- Aufdenkampe, Anthony K., Emilio Mayorga, Peter A. Raymond, John M. Melack, Scott C. Doney, Simone R. Alin, Rolf E. Aalto, and Kyungsoo Yoo. 2011. "Riverine Coupling of Biogeochemical Cycles between Land, Oceans, and Atmosphere." *Frontiers in Ecology and the Environment* 9 (1): 53–60. <https://doi.org/10.1890/100014>.
- Barthel, Matti, Marijn Bauters, Simon Baumgartner, Travis W. Drake, Nivens Mokwele Bey, Glenn Bush, Pascal Boeckx, et al. 2022. "Low N₂O and Variable CH₄ Fluxes from Tropical Forest Soils of the Congo Basin." *Nature Communications* 13 (1): 330. <https://doi.org/10.1038/s41467-022-27978-6>.
- Barton, Kamil. 2020. "MuMIn: Multi-Model Inference. R Package Version 1.43. 17."
- Bastviken, David, Lars J. Tranvik, John A. Downing, Patrick M. Crill, and Alex Enrich-Prast. 2011. "Freshwater Methane Emissions Offset the Continental Carbon Sink." *Science* 331 (6013): 50–50. <https://doi.org/10.1126/science.1196808>.
- Bates, Douglas, Martin Mächler, Ben Bolker, and Steve Walker. 2015. "Fitting Linear Mixed-Effects Models Using Lme4." *Journal of Statistical Software* 67 (October): 1–48. <https://doi.org/10.18637/jss.v067.i01>.
- Battin, Tom J., Ronny Lauerwald, Emily S. Bernhardt, Enrico Bertuzzo, Lluís Gómez Gener, Robert O. Hall, Erin R. Hotchkiss, et al. 2023. "River Ecosystem Metabolism and Carbon Biogeochemistry in a Changing World." *Nature* 613 (7944): 449–59. <https://doi.org/10.1038/s41586-022-05500-8>.
- Baumgartner, Simon, Matti Barthel, Travis W. Drake, Marijn Bauters, Isaac Ahanamungu Makelele, John Kalume Mugula, Laura Summerauer, Nora Gallarotti, Landry Cizungu Ntaboba, et al. 2020. "Seasonality, Drivers, and Isotopic Composition of Soil CO₂ & Sub<2> <2> Fluxes from Tropical Forests of the Congo Basin." Preprint. Biogeochemistry: Greenhouse Gases. <https://doi.org/10.5194/bg-2020-133>.
- Baumgartner, Simon, Matti Barthel, Travis William Drake, Marijn Bauters, Isaac Ahanamungu Makelele, John Kalume Mugula, Laura Summerauer, Nora Gallarotti, Landry Cizungu Ntaboba, et al. 2020. "Seasonality, Drivers, and Isotopic Composition of Soil CO₂ Fluxes from Tropical Forests of the Congo Basin." *Biogeosciences* 17 (23): 6207–18. <https://doi.org/10.5194/bg-17-6207-2020>.
- Borges, Alberto V., Gwenaél Abril, François Darchambeau, Cristian R. Teodoru, Jonathan Deborde, Luciana O. Vidal, Thibault Lambert, and Steven Bouillon. 2015. "Divergent Biophysical Controls of Aquatic CO₂ and CH₄ in the World's Two Largest Rivers." *Scientific Reports* 5: 1–10. <https://doi.org/10.1038/srep15614>.
- Borges, Alberto V., François Darchambeau, Thibault Lambert, Cedric Morana, George H. Allen, Ernest Tambwe, Alfred Toengaho Sembaito, et al. 2019. "Variations in Dissolved Greenhouse Gases (CO₂, CH₄, N₂O) in the Congo River Network Overwhelmingly Driven by Fluvial-Wetland Connectivity." *Biogeosciences* 16 (19): 3801–34. <https://doi.org/10.5194/bg-16-3801-2019>.
- Borges, Alberto V., François Darchambeau, Cristian R. Teodoru, Trent R. Marwick, Fredrick Tamoooh, Naomi Geeraert, Fredrick O. Omengo, et al. 2015. "Globally Significant Greenhouse-Gas Emissions from African Inland Waters." *Nature Geoscience* 8 (8): 637–42. <https://doi.org/10.1038/ngeo2486>.
- Borges Pinto, Osvaldo, George L. Vourlitis, Edna Maria De Souza Carneiro, Marizeth De França Dias, Cloe Hentz, and Jose De Souza Nogueira. 2018. "Interactions between Vegetation, Hydrology, and Litter Inputs on Decomposition and Soil CO₂ Efflux of Tropical Forests in the Brazilian Pantanal." *Forests* 9 (5): 281. <https://doi.org/10.3390/f9050281>.
- Bouillon, S., A. Yambélé, R. G. M. Spencer, D. P. Gillikin, P. J. Hernes, J. Six, R. Merckx, and A. V. Borges. 2012. "Organic Matter Sources, Fluxes and Greenhouse Gas Exchange in the Oubangui River (Congo River Basin)." *Biogeosciences* 9 (6): 2045–62. <https://doi.org/10.5194/bg-9-2045-2012>.
- Bréchet, Laëtitia M., Warren Daniel, Clément Stahl, Benoît Burban, Jean-Yves Goret, Roberto L. Salomón, and Ivan A. Janssens. 2021. "Simultaneous Tree Stem and Soil Greenhouse Gas (CO₂, CH₄, N₂O) Flux Measurements: A Novel

Formatted: French (Switzerland)

Design for Continuous Monitoring towards Improving Flux Estimates and Temporal Resolution.” *New Phytologist* 230 (6): 2487–2500. <https://doi.org/10.1111/nph.17352>.

Formatted: German (Switzerland)

- 580 Breitengroß, Jens Peter. 1972. “Saisonales Fließverhalten in Großflächigen Flußsystemen. Methoden Zur Erfassung Und Darstellung Am Beispiel Des Kongo (Zaire).” *Mitteilungen Der Geographischen Gesellschaft in Hamburg* 60: 1–92.
- Brooks, P. D., H. Geilmann, R. A. Werner, and W. A. Brand. 2003. “Improved Precision of Coupled $\Delta^{13}\text{C}$ and $\Delta^{15}\text{N}$ Measurements from Single Samples Using an Elemental Analyzer/Isotope Ratio Mass Spectrometer Combination with a Post-Column Six-Port Valve and Selective CO_2 Trapping; Improved Halide Robustness of the Combustion Reactor Using CeO_2 .” *Rapid Communications in Mass Spectrometry* 17 (16): 1924–26. <https://doi.org/10.1002/rcm.1134>.
- 585 Buchmann, N., J.-M. Guehl, T. S. Barigah, and J. R. Ehleringer. 1997. “Interseasonal Comparison of CO_2 Concentrations, Isotopic Composition, and Carbon Dynamics in an Amazonian Rainforest (French Guiana).” *Oecologia* 110 (1): 120–31. <https://doi.org/10.1007/s004420050140>.
- 590 Conrad, Ralf, Pengfei Liu, and Peter Claus. 2021. “Fractionation of Stable Carbon Isotopes during Acetate Consumption by Methanogenic and Sulfidogenic Microbial Communities in Rice Paddy Soils and Lake Sediments.” *Biogeosciences* 18 (24): 6533–46. <https://doi.org/10.5194/bg-18-6533-2021>.
- Courtois, Elodie A., Clément Stahl, Joke Van den Berge, Laëtitia Bréchet, Leandro Van Langenhove, Andreas Richter, Ifigenia Urbina, Jennifer L. Soong, Josep Peñuelas, and Ivan A. Janssens. 2018. “Spatial Variation of Soil CO_2 , CH_4 and N_2O Fluxes Across Topographical Positions in Tropical Forests of the Guiana Shield.” *Ecosystems* 21 (7): 1445–58. <https://doi.org/10.1007/s10021-018-0232-6>.
- 595 Crezee, Bart, Greta C. Dargie, Corneille E. N. Ewango, Edward T. A. Mitchard, Ovide Emba B., Joseph Kanyama T., Pierre Bola, et al. 2022. “Mapping Peat Thickness and Carbon Stocks of the Central Congo Basin Using Field Data.” *Nature Geoscience* 15 (8): 639–44. <https://doi.org/10.1038/s41561-022-00966-7>.
- 600 Daelman, Roxanne, Marijn Bauters, Matti Barthel, Emmanuel Bulonza, Lodewijk Lefevre, José Mbifo, Johan Six, et al. 2024. “Spatiotemporal Variability of CO_2 , N_2O and CH_4 Fluxes from a Semi-Deciduous Tropical Forest Soil in the Congo Basin.” *EGU sphere*, August, 1–21. <https://doi.org/10.5194/egusphere-2024-2346>.
- Dalmagro, Higo J., Michael J. Lathuillière, Iain Hawthorne, Douglas D. Morais, Osvaldo B. Pinto Jr, Eduardo G. Couto, and Mark S. Johnson. 2018. “Carbon Biogeochemistry of a Flooded Pantanal Forest over Three Annual Flood Cycles.” *Biogeochemistry* 139 (1): 1–18. <https://doi.org/10.1007/s10533-018-0450-1>.
- 605 Davidson, Eric A., Françoise Yoko Ishida, and Daniel C. Nepstad. 2004. “Effects of an Experimental Drought on Soil Emissions of Carbon Dioxide, Methane, Nitrous Oxide, and Nitric Oxide in a Moist Tropical Forest.” *Global Change Biology* 10 (5): 718–30. <https://doi.org/10.1111/j.1365-2486.2004.00762.x>.
- Docherty, Emma M., and Andrew D. Thomas. 2021. “Larger Floods Reduce Soil CO_2 Efflux during the Post-Flooding Phase in Seasonally-Flooded Forests of Western Amazonia.” *Pedosphere* 31 (2): 342–52. [https://doi.org/10.1016/S1002-0160\(20\)60073-X](https://doi.org/10.1016/S1002-0160(20)60073-X).
- 610 Doff sotta, Eleneide, Patrick Meir, Yadvinder Malhi, Antonio Donato nobre, Martin Hodnett, and John Grace. 2004. “Soil CO_2 Efflux in a Tropical Forest in the Central Amazon.” *Global Change Biology* 10 (5): 601–17. <https://doi.org/10.1111/j.1529-8817.2003.00761.x>.
- 615 Drake, Travis W., Matti Barthel, Christian Ekemba Mbongo, Davin Mata Mpambi, Simon Baumgartner, Clement Ikene Botefa, Marijn Bauters, et al. 2023. “Hydrology Drives Export and Composition of Carbon in a Pristine Tropical River.” *Limnology and Oceanography* 68 (11): 2476–91. <https://doi.org/10.1002/lno.12436>.
- Drake, Travis W., Peter A. Raymond, and Robert G. M. Spencer. 2018. “Terrestrial Carbon Inputs to Inland Waters: A Current Synthesis of Estimates and Uncertainty.” *Limnology and Oceanography Letters* 3 (3): 132–42. <https://doi.org/10.1002/lol2.10055>.
- 620 Epron, Daniel, Yann Nouvellon, Louis Mareschal, Rildo Moreira e Moreira, Lydie-Stella Koutika, Blandine Geneste, Juan Sinfioriano Delgado-Rojas, et al. 2013. “Partitioning of Net Primary Production in Eucalyptus and Acacia Stands and in Mixed-Species Plantations: Two Case-Studies in Contrasting Tropical Environments.” *Forest Ecology and Management* 301 (August): 102–11. <https://doi.org/10.1016/j.foreco.2012.10.034>.
- 625 Gallarotti, Nora, Matti Barthel, Elizabeth Verhoeven, Engil Isadora Pujol Pereira, Marijn Bauters, Simon Baumgartner, Travis W. Drake, et al. 2021. “In-Depth Analysis of N_2O Fluxes in Tropical Forest Soils of the Congo Basin Combining

Isotope and Functional Gene Analysis.” *ISME Journal* 15 (11): 3357–74. <https://doi.org/10.1038/s41396-021-01004-x>.

630 Garcia-Montiel, Diana C., Jerry M. Melillo, Paul A. Steudler, Hanqin Tian, Christopher Neill, David W. Kicklighter, Brigitte Feigl, Marisa Piccolo, and Carlos C. Cerri. 2004. “Emissions of N₂o and Co₂ from Terra Firme Forests in Rondônia, Brazil.” *Ecological Applications* 14 (sp4): 214–20. <https://doi.org/10.1890/01-6023>.

Georgiou, Selena, Edward T. A. Mitchard, Bart Crezee, Greta C. Dargie, Dylan M. Young, Antonio J. Jovani-Sancho, Benjamin Kitambo, et al. 2023. “Mapping Water Levels across a Region of the Cuvette Centrale Peatland Complex.” *Remote Sensing* 15 (12): 3099. <https://doi.org/10.3390/rs15123099>.

635 Goodrick, I., S. Connor, M. I. Bird, and P. N. Nelson. 2016. “Emission of CO₂ from Tropical Riparian Forest Soil Is Controlled by Soil Temperature, Soil Water Content and Depth to Water Table.” *Soil Research* 54 (3): 311. <https://doi.org/10.1071/SR15040>.

Grolemund, Garrett, and Hadley Wickham. 2011. “Dates and Times Made Easy with Lubridate.” *Journal of Statistical Software* 40 (3): 1–25. <https://doi.org/10.18637/jss.v040.i03>.

640 Hashimoto, S, N Carvalhais, A Ito, M Migliavacca, K Nishina, and M Reichstein. 2015. “Global Spatiotemporal Distribution of Soil Respiration Modeled Using a Global Database.”

Hotchkiss, E. R., R. O. Hall Jr, R. A. Sponseller, D. Butman, J. Klaminder, H. Laudon, M. Rosvall, and J. Karlsson. 2015. “Sources of and Processes Controlling CO₂ Emissions Change with the Size of Streams and Rivers.” *Nature Geoscience* 8 (9): 696–99. <https://doi.org/10.1038/ngeo2507>.

645 Huang, Ni, Li Wang, Xiao-Peng Song, T. Andrew Black, and Zheng Niu. 2020. “Spatial and Temporal Variations in Global Soil Respiration and Their Relationships with Climate and Land Cover.” <https://doi.org/10.1126/sciadv.abb8508>.

Hubau, Wannes, Simon L. Lewis, Oliver L. Phillips, Kofi Affum-Baffoe, Hans Beeckman, Aida Cuní-Sanchez, Armandu K. Daniels, et al. 2020. “Asynchronous Carbon Sink Saturation in African and Amazonian Tropical Forests.” *Nature* 579 (7797): 80–87. <https://doi.org/10.1038/s41586-020-2035-0>.

650 Janssens, Ivan A., S. Tété Barigah, and Reinhart Ceulemans. 1998. “Soil CO₂ Efflux Rates in Different Tropical Vegetation Types in French Guiana.” *Annales Des Sciences Forestières* 55 (6): 671–80. <https://doi.org/10.1051/forest:19980603>.

Jian, J., Vargas, R., Anderson-Teixeira, K.J., Stell, E., Herrmann, V., Horn, M., Kholod, N., et al. 2021. “Soil CollectionA Global Database of Soil Respiration Data, Version 5.0.” CSV, 0 MB. <https://doi.org/10.3334/ORNLDAAAC/1827>.

655 Katayama, Ayumi, Tomonori Kume, Hikaru Komatsu, Mizue Ohashi, Michiko Nakagawa, Megumi Yamashita, Kyoichi Otsuki, Masakazu Suzuki, and Tomo’omi Kumagai. 2009. “Effect of Forest Structure on the Spatial Variation in Soil Respiration in a Bornean Tropical Rainforest.” *Agricultural and Forest Meteorology* 149 (10): 1666–73. <https://doi.org/10.1016/j.agrformet.2009.05.007>.

Keeling, D. 1958. “The Concentration and Isotopic Abundances of Atmospheric Carbon Dioxide in Rural Areas.” *Geochimica et Cosmochimica Acta* 13: 322–34.

660 Kuznetsova, Alexandra, Per B. Brockhoff, and Rune H. B. Christensen. 2017. “LmerTest Package: Tests in Linear Mixed Effects Models.” *Journal of Statistical Software* 82 (13). <https://doi.org/10.18637/jss.v082.i13>.

Kuzyakov, Yakov, and Olga Gavrichkova. 2010. “REVIEW: Time Lag between Photosynthesis and Carbon Dioxide Efflux from Soil: A Review of Mechanisms and Controls.” *Global Change Biology* 16 (12): 3386–3406. <https://doi.org/10.1111/j.1365-2486.2010.02179.x>.

665 Lewis, Simon L., Bonaventure Sonké, Terry Sunderland, Serge K. Begne, Gabriela Lopez-Gonzalez, Geertje M. F. van der Heijden, Oliver L. Phillips, et al. 2013. “Above-Ground Biomass and Structure of 260 African Tropical Forests.” *Philosophical Transactions of the Royal Society B: Biological Sciences* 368 (1625): 20120295. <https://doi.org/10.1098/rstb.2012.0295>.

Lüdecke, Daniel. 2013. “SjPlot: Data Visualization for Statistics in Social Science.” Comprehensive R Archive Network. <https://doi.org/10.32614/CRAN.package.sjPlot>.

670 Mann, P. J., R. G. M. Spencer, B. J. Dinga, J. R. Poulsen, P. J. Hernes, G. Fiske, M. E. Salter, et al. 2014. “The Biogeochemistry of Carbon across a Gradient of Streams and Rivers within the Congo Basin.” *Journal of Geophysical Research: Biogeosciences* 119 (4): 687–702. <https://doi.org/10.1002/2013JG002442>.

675 Mann, Paul J., R. G. M. Spencer, B. J. Dinga, J. R. Poulsen, P. J. Hernes, G. Fiske, M. E. Salter, et al. 2014. “The Biogeochemistry of Carbon across a Gradient of Streams and Rivers within the Congo Basin.” *Journal of Geophysical Research: Biogeosciences* 119 (4): 687–702. <https://doi.org/10.1002/2013JG002442>.

Formatted: French (Switzerland)

Formatted: French (Switzerland)

- Mann, Paul J., Malak M Tfaily, William T Cooper, Joel E Kostka, Patrick R Chanton, Christopher W Schadt, Paul J Hanson, Colleen M Iversen, Jeffrey P Chanton, and Paul J. Mann. 2014. "Journal of Geophysical Research: Biogeosciences." *Journal of Geophysical Research: Biogeosciences*, 661–75. <https://doi.org/10.1002/2013JG002442>.Received.
- 680 Mitchard, Edward T. A. 2018. "The Tropical Forest Carbon Cycle and Climate Change." *Nature* 559 (7715): 527–34. <https://doi.org/10.1038/s41586-018-0300-2>.
- Nakagawa, Shinichi, Paul C. D. Johnson, and Holger Schielzeth. 2017. "The Coefficient of Determination R² and Intra-Class Correlation Coefficient from Generalized Linear Mixed-Effects Models Revisited and Expanded." *Journal of the Royal Society, Interface* 14 (134): 20170213. <https://doi.org/10.1098/rsif.2017.0213>.
- 685 Nissan, Alon, Uria Alcolombri, Nadav Peleg, Nir Galili, Joaquin Jimenez-Martinez, Peter Molnar, and Markus Holzner. 2023. "Global Warming Accelerates Soil Heterotrophic Respiration." *Nature Communications* 14 (1): 3452. <https://doi.org/10.1038/s41467-023-38981-w>.
- Oertel, Cornelius, Jörg Matschullat, Kamal Zurba, Frank Zimmermann, and Stefan Erasmi. 2016. "Greenhouse Gas Emissions from Soils—A Review." *Chemie Der Erde - Geochemistry* 76 (April). <https://doi.org/10.1016/j.chemer.2016.04.002>.
- 690 Ohashi, Mizue, Tomonori Kume, Seiki Yamane, and Masakazu Suzuki. 2007. "Hot Spots of Soil Respiration in an Asian Tropical Rainforest." *Geophysical Research Letters* 34 (8). <https://doi.org/10.1029/2007GL029587>.
- Parmentier, Ingrid, Yadvinder Malhi, Bruno Senterre, Robert J. Whittaker, Alfonso and ALONSO, Michael P. B. Balinga, Adama Bakayoko, et al. 2007. "The Odd Man out? Might Climate Explain the Lower Tree α -Diversity of African Rain Forests Relative to Amazonian Rain Forests?" *Journal of Ecology* 95 (5): 1058–71. <https://doi.org/10.1111/j.1365-2745.2007.01273.x>.
- 695 Pavelka, Marian, Manuel Acosta, Ralf Kiese, N ria Altimir, Christian Br mmer, Patrick Crill, Eva Darenova, et al. 2018. "Standardisation of Chamber Technique for CO₂, N₂O and CH₄ Fluxes Measurements from Terrestrial Ecosystems." *International Agrophysics* 32 (4): 569–87. <https://doi.org/10.1515/intag-2017-0045>.
- Pelletier, Luc, Ian B. Strachan, Michelle Garneau, and Nigel T. Roulet. 2014. "Carbon Release from Boreal Peatland Open Water Pools: Implication for the Contemporary C Exchange." *Journal of Geophysical Research: Biogeosciences* 119 (3): 207–22. <https://doi.org/10.1002/2013JG002423>.
- 700 R Core Team. 2023. "R: A Language and Environment for Statistical Computing." Vienna, Austria.
- Rasera, Maria de F tima F. L., Maria Victoria R. Ballester, Alex V. Krusche, Cleber Salimon, L ticia A. Montebelo, Simone R. Alin, Reynaldo L. Victoria, and Jeffrey E. Richey. 2008. "Estimating the Surface Area of Small Rivers in the Southwestern Amazon and Their Role in CO₂ Outgassing." *Earth Interactions* 12 (6): 1–16. <https://doi.org/10.1175/2008EI257.1>.
- 705 Raymond, Peter A., Jens Hartmann, Ronny Lauerwald, Sebastian Sobek, Cory McDonald, Mark Hoover, David Butman, et al. 2013. "Global Carbon Dioxide Emissions from Inland Waters." *Nature* 503 (7476): 355–59. <https://doi.org/10.1038/nature12760>.
- 710 Rocher-Ros, Gerard, Ryan A. Sponseller, William Lidberg, Carl-Magnus M rth, and Reiner Giesler. 2019. "Landscape Process Domains Drive Patterns of CO₂ Evasion from River Networks." *Limnology and Oceanography Letters* 4 (4): 87–95. <https://doi.org/10.1002/lol2.10108>.
- Rosentreter, Judith A., Alberto V. Borges, Bridget R. Deemer, Meredith A. Holgerson, Shaoda Liu, Chunlin Song, John Melack, et al. 2021. "Half of Global Methane Emissions Come from Highly Variable Aquatic Ecosystem Sources." *Nature Geoscience* 14 (4): 225–30. <https://doi.org/10.1038/s41561-021-00715-2>.
- 715 RStudio Team. 2023. "RStudio: Integrated Development Environment for R." Boston, MA.
- Rubio, Vanessa E., and Matteo Detto. 2017. "Spatiotemporal Variability of Soil Respiration in a Seasonal Tropical Forest." *Ecology and Evolution* 7 (17): 7104–16. <https://doi.org/10.1002/ece3.3267>.
- 720 Runge, J. 2007. "The Congo River, Central Africa." In *Large Rivers: Geomorphology and Management*, edited by Avijit Gupta, 1st ed., 293–308. West Sussex: John Wiley & Sons, Ltd.
- Scofield, Vinicius, John M. Melack, Pedro M. Barbosa, Jo o Henrique F. Amaral, Bruce R. Forsberg, and Vinicius F. Farjalla. 2016. "Carbon Dioxide Outgassing from Amazonian Aquatic Ecosystems in the Negro River Basin." *Biogeochemistry* 129 (1): 77–91. <https://doi.org/10.1007/s10533-016-0220-x>.
- 725 Slik, J. W. Ferry, V ctor Arroyo-Rodr guez, Shin-Ichiro Aiba, Patricia Alvarez-Loayza, Luciana F. Alves, Peter Ashton, Patricia Balvanera, et al. 2015. "An Estimate of the Number of Tropical Tree Species." *Proceedings of the National Academy of Sciences* 112 (24): 7472–77. <https://doi.org/10.1073/pnas.1423147112>.

Formatted: German (Switzerland)

- Sotta, E. D., E. Veldkamp, Luitgard Schwendenmann, B. R. Guimarães, R. K. Paixão, Mdlp Ruivo, A. C. Lola Da Costa, and P. Meir. 2007. "Effects of an Induced Drought on Soil Carbon Dioxide (CO₂) Efflux and Soil CO₂ Production in an Eastern Amazonian Rainforest, Brazil," October. <https://researchspace.auckland.ac.nz/handle/2292/30543>.
- 730 Sousa Neto, E., J. B. Carmo, M. Keller, S. C. Martins, L. F. Alves, S. A. Vieira, M. C. Piccolo, et al. 2011. "Soil-Atmosphere Exchange of Nitrous Oxide, Methane and Carbon Dioxide in a Gradient of Elevation in the Coastal Brazilian Atlantic Forest." *Biogeosciences* 8 (3): 733–42. <https://doi.org/10.5194/bg-8-733-2011>.
- Stoffel, Martin A., Shinichi Nakagawa, and Holger Schielzeth. 2021. "PartR2: Partitioning R2 in Generalized Linear Mixed Models." *PeerJ* 9 (May): e11414. <https://doi.org/10.7717/peerj.11414>.
- 735 Tathy, J. P., B. Cros, R. A. Delmas, A. Marengo, J. Servant, and M. Labat. 1992. "Methane Emission from Flooded Forest in Central Africa." *Journal of Geophysical Research: Atmospheres* 97 (D6): 6159–68. <https://doi.org/10.1029/90JD02555>.
- Upstill-Goddard, Robert C., Matthew E. Salter, Paul J. Mann, Jonathan Barnes, John Poulsen, Bienvenu Dinga, Gregory J. Fiske, and Robert M. Holmes. 2017. "The Riverine Source of CH₄ and N₂O from the Republic of Congo, Western Congo Basin." *Biogeosciences* 14 (9): 2267–81. <https://doi.org/10.5194/bg-14-2267-2017>.
- 740 Verchot, Louis V., Michael Dannenmann, Steve Kwatcho Kengdo, Charles Baudouin Njine-Bememba, Mariana C. Rufino, Denis Jean Sonwa, and Javier Tejedor. 2020. "Land-Use Change and Biogeochemical Controls of Soil CO₂, N₂O and CH₄ Fluxes in Cameroonian Forest Landscapes." *Journal of Integrative Environmental Sciences*, December. <https://www.tandfonline.com/doi/abs/10.1080/1943815X.2020.1779092>.
- 745 Wanninkhof, Rik. 2014. "Relationship between Wind Speed and Gas Exchange over the Ocean Revisited." *Limnology and Oceanography: Methods* 12 (6): 351–62. <https://doi.org/10.4319/lom.2014.12.351>.
- Werner, Christian, Ralf Kiese, and Klaus Butterbach-Bahl. 2007. "Soil-Atmosphere Exchange of N₂O, CH₄, and CO₂ and Controlling Environmental Factors for Tropical Rain Forest Sites in Western Kenya." *Journal of Geophysical Research: Atmospheres* 112 (D3). <https://doi.org/10.1029/2006JD007388>.
- 750 Werner, Roland A., and Willi A. Brand. 2001. "Referencing Strategies and Techniques in Stable Isotope Ratio Analysis." *Rapid Communications in Mass Spectrometry* 15 (7): 501–19. <https://doi.org/10.1002/rcm.258>.
- Werner, Roland A., Beate A. Bruch, and Willi A. Brand. 1999. "ConFlo III – an Interface for High Precision $\Delta^{13}\text{C}$ and $\Delta^{15}\text{N}$ Analysis with an Extended Dynamic Range." *Rapid Communications in Mass Spectrometry* 13 (13): 1237–41. [https://doi.org/10.1002/\(SICI\)1097-0231\(19990715\)13:13<1237::AID-RCM633>3.0.CO;2-C](https://doi.org/10.1002/(SICI)1097-0231(19990715)13:13<1237::AID-RCM633>3.0.CO;2-C).
- 755 Werner, Roland A., Michael Rothe, and Willi A. Brand. 2001. "Extraction of CO₂ from Air Samples for Isotopic Analysis and Limits to Ultra High Precision $\Delta^{18}\text{O}$ Determination in CO₂ Gas." *Rapid Communications in Mass Spectrometry* 15 (22): 2152–67. <https://doi.org/10.1002/rcm.487>.
- Wickham, Hadley. 2009. *Ggplot2*. New York, NY: Springer New York. <https://doi.org/10.1007/978-0-387-98141-3>.
- 760 Wickham, Hadley, Romain François, Lionel Henry, Kirill Müller, and Davis Vaughan. 2023. "Dplyr: A Grammar of Data Manipulation." *R Package Version 1.1.4*.
- Wild, Jan, Martin Kopecký, Martin Macek, Martin Šanda, Jakub Jankovec, and Tomáš Haase. 2019. "Climate at Ecologically Relevant Scales: A New Temperature and Soil Moisture Logger for Long-Term Microclimate Measurement." *Agricultural and Forest Meteorology* 268 (April): 40–47. <https://doi.org/10.1016/j.agrformet.2018.12.018>.
- 765 Zanchi, Fabrício Berton, Maarten Johannes Waterloo, Albertus Johannes Dolman, Margriet Groenendijk, Jürgen Kesselmeier, Bart Kruijt, Marcos Alexandre Bolson, Flávio Jesus Luizão, and Antônio Ocimar Manzi. 2011. "Influence of Drainage Status on Soil and Water Chemistry, Litter Decomposition and Soil Respiration in Central Amazonian Forests on Sandy Soils." *Ambiente e Agua - An Interdisciplinary Journal of Applied Science* 6 (1): 6–29. <https://doi.org/10.4136/ambi-agua.170>.

Formatted: French (Switzerland)